

See discussions, stats, and author profiles for this publication at: <https://www.researchgate.net/publication/226870387>

Carbon Nanotubes as Electrical Interfaces with Neurons

Chapter · February 2010

DOI: 10.1007/978-90-481-8553-5_11

CITATIONS

6

READS

218

2 authors:



William Lee

18 PUBLICATIONS 426 CITATIONS

SEE PROFILE



Vladimir Parpura

University of Alabama at Birmingham

263 PUBLICATIONS 17,363 CITATIONS

SEE PROFILE

Some of the authors of this publication are also working on these related projects:



The hypothalamo-neurohypophysial system and its translational potential [View project](#)

01 **Chapter 11**
02 **Carbon Nanotubes as Electrical Interfaces**
03 **with Neurons**
04
05
06

07 **William Lee and Vladimir Parpura**
08
09
10
11
12

13 **Abstract** Carbon nanotubes (CNTs) are emerging as promising nanomaterials for
14 biomedical applications. Due to their unique structural, mechanical and electronic
15 properties, CNTs can be used as electrical interfaces with the brain in particular
16 with neurons. CNT-based neural interfaces/electrodes have been employed in cell
17 culture and in vivo; they offer advantages over standard metal-based electrodes in
18 terms of monitoring and stimulation of neuronal activity. One of the challenges for
19 interfacing brain and machine is the biocompatibility of the materials used for elec-
20 trode construction. While CNTs appear biocompatible, the exposure limits have not
21 been set thus far. An appropriate (inter)national standards/rules for the use of CNTs
22 need to be established before CNT-based electrodes/devices can be used in human
23 subjects.
24
25

26 **Abbreviations**
27

28	BBB	blood-brain barrier
29	CNTs	carbon nanotubes
30	DRG	dorsal root ganglion
31	EEG	electroencephalogram
32	ERP	event-related potentials
33	MEA	microelectrode array
34	MWNTs	multi-walled CNTs
35	PPy	polypyrrole
36	RGCs	retinal ganglion cells
37	SWNTs	single-walled CNTs
38	TiN	titanium nitride

39
40

41 V. Parpura (✉)
42 Department of Neurobiology, Center for Glial Biology in Medicine, Atomic Force
43 Microscopy & Nanotechnology Laboratories, Civitan International Research Center,
44 Evelyn F. McKnight Brain Institute, University of Alabama, Birmingham, AL, USA
45 e-mail: vlad@uab.edu

46 VACNFs vertically aligned carbon nanofibers
47 3D three-dimensional
48
49

50 11.1 Introduction

51
52 Carbon nanotubes (CNTs) are emerging as one of the most promising nanomaterials for applications in electronics, aerospace and biomedicine. In this chapter we discuss the use of CNTs as electrical interfaces with the brain in particular with its electrically excitable cellular components, neurons. We begin with a primer on CNTs unique structural, mechanical and electronic properties, which have captured the attention of physicists, chemists and material scientists and prompt the use of CNTs in biomedical applications (Section 11.2). This is followed by a discussion of a subset of experimental approaches using CNT-based neural interfaces in cell culture and in vivo to illustrate the advantages that CNTs can offer over standard metal-based electrodes in terms of monitoring and stimulation of neuronal activity (Section 11.3). Finally, we briefly discuss biosafety of CNTs and raise the concern as to the lack of exposure limit guidance to date (Section 11.4).
53
54
55
56
57
58
59
60
61
62
63
64
65

66 11.2 Primer on Characteristics of CNTs

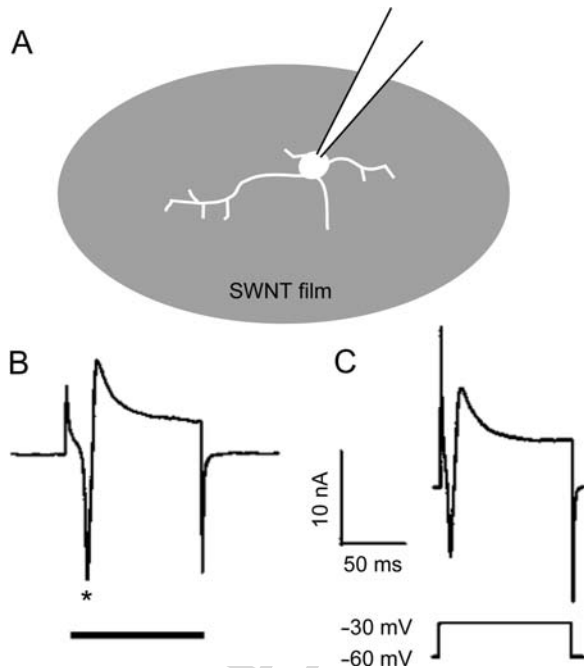
67
68 Detailed description of the structure, properties and modification/functionalization of CNTs is available elsewhere [1, 2]. Briefly, CNTs are composed of graphene sheets rolled into cylinders, which have a hollow core. The cylindrical ends can be capped with a fullerene dome. Based on the number of concentric graphene cylinders within CNTs, they are classified into single-walled CNTs (SWNTs), double-walled CNTs, or multi-walled CNTs (MWNT). SWNTs commonly have their diameters between 0.7 and 2 nm, although their diameter down to 0.4 nm have been reported [3, 4]. MWNTs have an outer diameter that typically ranges from 2 to 100 nm, while the inner diameter varies between 1 and 3 nm. The length of synthesized CNTs is typically in the μm range, although SWNTs up to 4 cm have been reported [5]. CNTs have an exceptional mechanical strength with a Young's modulus of ~ 1 TPa. They are chemically relatively inert and non-biodegradable. In addition, CNTs exhibit unique electrical properties. CNT conductivity is endowed by the conformation of their hexagonal graphene lattice, which can be arm-chair, zig-zag, or chiral. They can be metallic or semi-conductive. In metallic CNTs, the graphene hexagonal lattice can be arranged in any of the three configurations, with all arm-chair CNTs being metallic. In semi-conductive CNTs, the lattice can be arranged in a zig-zag or chiral configuration. The combined physical properties make CNTs a durable nanomaterial for bio-engineering, especially in applications where a sustained presence of the material is desirable, such as stimulation/recording electrodes for interface with neural elements as discussed below.
69
70
71
72
73
74
75
76
77
78
79
80
81
82
83
84
85
86
87
88
89
90

11.3 CNT-Based Neural Interfaces for Stimulation and Monitoring of Neuronal Activity

An in-depth review on neural stimulation/recording electrodes is available elsewhere [6]. One of the challenges in designing electrodes for neural interfaces is to maximize delivery of electrical stimulation to cells with high selectivity, while minimizing tissue damage. In recording mode, electrodes with high sensitivity, as evidenced by high signal to noise ratio, are desirable. Amongst the nanomaterials available to date, CNTs display desirable properties for use in stimulation/recording electrodes. (i) CNT-based electrodes have been successfully miniaturized while they do not seem to inflict tissue damage. (ii) CNTs have the ability to operate as ballistic conductors which aids in lowering impedance and increasing charge transfer. (iii) CNTs display exceptional flexibility and they can be twisted and bent to a large degree, although they are five times mechanically stronger than steel [7]. These traits are advantageous for materials to be used for microelectrodes that would penetrate through the tissue. Such properties of CNTs allowed for their use in stimulating and monitoring of neuronal activity at various levels of spatial domains [see definition of levels in Ref. [8]], which includes (i) stimulation of action potentials/ Ca^{2+} excitability in a small group of neurons in culture using CNT films of multi-electrode arrays, (ii) stimulating and recording from neurons in hippocampal organotypic slice cultures as well and in the whole mount mouse retina, (iii) stimulation of and recording from rat and monkey cortices, and (iv) recording human electroencephalogram (EEG) through a CNT-based attachment to the superficial skin layer. We describe below a subset of experimental approaches demonstrating such usage of CNTs.

Liopo et al. [9] demonstrated the ability to electrically stimulate neural cells directly through a CNT substrate. In this study, the neuroblastoma x glioma NG108 cell line or rat dorsal root ganglion (DRG) cells were cultured on planar and transparent SWNT films deposited onto overhead transparencies, i.e. polyethylene terephthalate sheets (Fig. 11.1a). NG108 cells and DRG neurons were subjected to electrophysiological recordings using a whole-cell patch clamp configuration to monitor the electrical activity of individual cells. These cells were then electrically stimulated either via a patch pipette or through a conductive SWNT film (Fig. 11.1b and c). Recorded currents due to two different stimulation methods appear qualitatively similar, indicating that an SWNT film can be used as a stimulation platform. Subsequent studies have demonstrated that various planar CNT films can be used for cellular growth and direct electrical stimulation of cultured primary neurons [10, 11], NG108 cells [12] and differentiated neural stem cells [13]. The ability of CNTs to deliver electrical stimulation to neurons can be attributed to their conductivity and their intimate contacts with neurons as revealed by electron microscopy [10–12, 14]. It should be noted, however, that while whole-cell patch clamp allows stimulating the same cell that is recorded from, CNT film stimulation excites the entire population of cells that are residing on the film which also serves as a planar growth scaffold/substrate. Since CNTs films/deposition is amenable to miniaturization, one possible solution for achieving the use of CNTs for

136 **Fig. 11.1** Electrical
 137 stimulation of dorsal root
 138 ganglion (DRG) neurons via
 139 a planar SWNT film.
 140 (a) Schematic representation
 141 of an experimental setup.
 142 DGR neurons grown on
 143 SWNT films (grey) were
 144 subjected to
 145 electrophysiological
 146 recordings using a whole-cell
 147 patch clamp configuration.
 148 (b) Stimulation (direct
 149 current, *horizontal bar*) of a
 150 DRG neuron through the
 151 SWNT film causes an inward
 152 current (*asterisk*), similar to
 153 that seen when voltage steps
 154 were applied via a patch
 155 pipette (c). (b–c) Modified
 156 from [9], with permission



160 recording/stimulation of individual neurons, or a small group of these cells, within
 161 the network is to generate a so-called microelectrode array (MEA).

162 Wang et al. [15] developed a CNT-based MEA comprised of pillars made of vertically
 163 aligned conductive MWNTs (Fig. 11.2). The size, the geometry and location
 164 of the CNT pillars can be precisely controlled by lithography. CNT pillars electro-
 165 des have rectangular ($30 \times 30 \mu\text{m}$, $50 \times 50 \mu\text{m}$, or $100 \times 100 \mu\text{m}$) or circular
 166 ($50 \mu\text{m}$ in diameter) geometry with a height of $40 \mu\text{m}$ (Fig. 11.2a–c). Pillars were
 167 integrated onto a pre-patterned microcircuit and they were individually address-
 168 able. These electrodes have high charge injection capacity and operate without
 169 faradic/electrochemical reactions, that otherwise can lead to irreversible damage of
 170 the electrodes and surrounding tissue. Thus, they represent a prototype for efficient
 171 and biocompatible interfacing for neural prosthesis. Indeed, the authors demon-
 172 strated a potential of the MEA approach for neuronal stimulation by using cultured
 173 neurons. Dissociated hippocampal neurons were plated onto MEAs. Cells displayed
 174 viability and neurite outgrowth consistent with the previously shown biocompatibil-
 175 ity of MWNTs [16, 17]. Rather than directly recording electrical activity of neurons,
 176 the authors assessed neuronal intracellular Ca^{2+} excitability due to electrical stim-
 177 ulation via CNT pillars. For dynamic Ca^{2+} imaging a fluorescent Ca^{2+} indicator
 178 was used. Since an inverted microscope was used while CNTs were nontransparent,
 179 the fluorescence emission from cells directly on the CNT pads could not be
 180 visualized. However, neurons that were in near proximity of stimulating electrodes

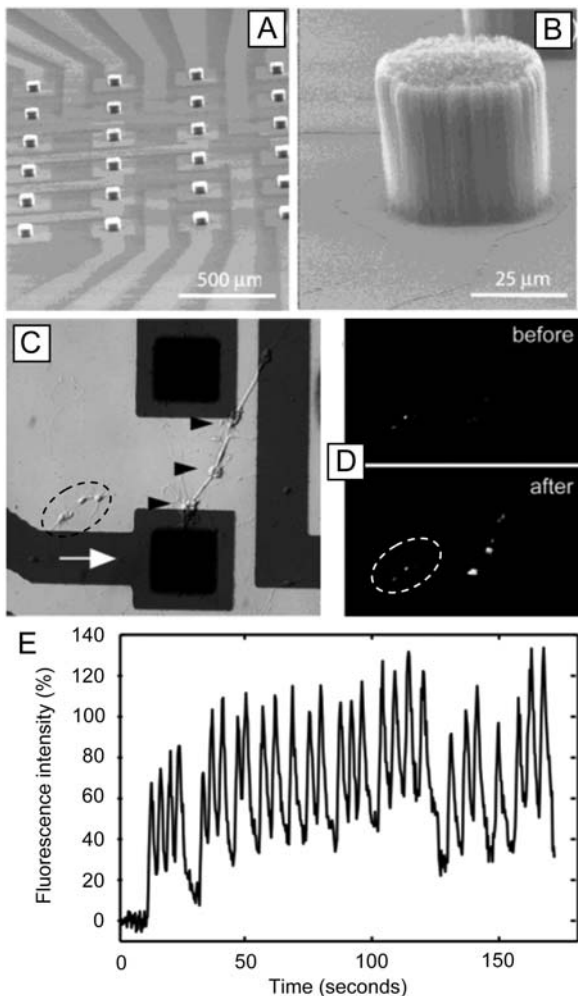
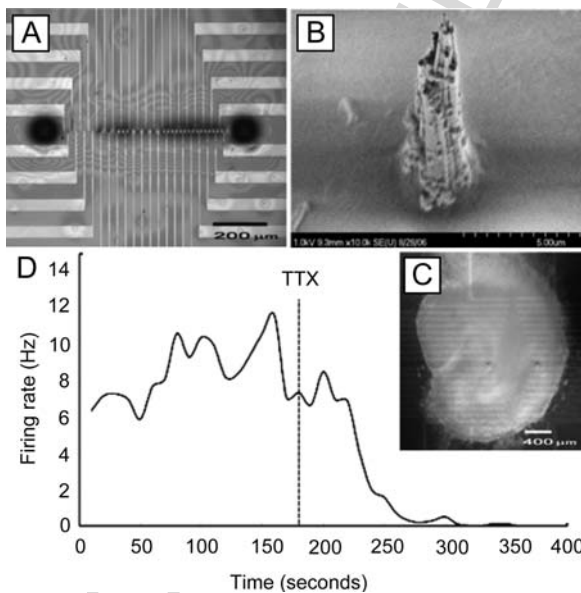


Fig. 11.2 Electrical stimulation of hippocampal neurons grown on an MWNT-based micro-electrode array (MEA). (a) CNT-based MEA comprised of pillars made of vertically aligned conductive MWNTs and having either rectangular ($30 \times 30 \mu\text{m}$) or (b) circular ($50 \mu\text{m}$ in diameter) geometry with a height of $40 \mu\text{m}$. (c) Pillars are integrated onto a pre-patterned microcircuit and they are individually addressable. Hippocampal neurons grown on MEA ($100 \times 100 \mu\text{m}$ pillars) were electrically stimulated (*white arrow*). (d) Neurons loaded with a fluorescent Ca^{2+} indicator before and after electrical stimulation, which causes the increase in intracellular Ca^{2+} levels in neurons in contact with each other and a CNT pillar (*black arrowheads* in c). Note that neurons that were not in contact with CNT pillars show no changes in intracellular Ca^{2+} excitability (*left, dashed oval*; also see c). (e) Time course of intracellular Ca^{2+} dynamics due to repetitive cell stimulation. Modified from [15], with permission

226 showed increases in intracellular Ca^{2+} levels seen as the increase in the fluorescence
 227 intensity (Fig. 11.2d). Repeated stimulation paradigm caused transient increases in
 228 intracellular Ca^{2+} levels (Fig. 11.2e). In contrast, neurons that were not in contact
 229 with CNT pillars show no changes in intracellular Ca^{2+} excitability. Taken together,
 230 these experiments show that MEA made out of CNTs have potential for use in tissue
 231 and show promise as bio-compatible and efficient electrodes.

232 Yu et al. [18] used vertically aligned carbon nanofibers (VACNFs), a form of
 233 carbon material closely related to MWNTs, to generate MEAs which they utilized
 234 to stimulate neurons and record from these cells in cultured organotypic hippocam-
 235 pal slices. In this study, 40 individually addressable VACNF electrodes, 10 μm in
 236 height and spaced 15 μm apart, were arranged in a linear array with a total length of
 237 600 μm (Fig. 11.3a). Individual VACNF electrodes assumed a cone-like geometry,
 238 which aids their penetration of the tissue leading to improved electrical interface
 239 with neurons (Fig. 11.3b). VACNF electrodes had effective radius of up to $\sim 17 \mu\text{m}$
 240 [see Fig. 2 in Ref. [18]]. Although such size of VACNF electrodes is smaller than
 241 traditional metal surface electrodes, the electrical noise level recorded for VACNFs
 242 electrodes was comparable to that of various metal-based MEAs reported elsewhere
 243
 244

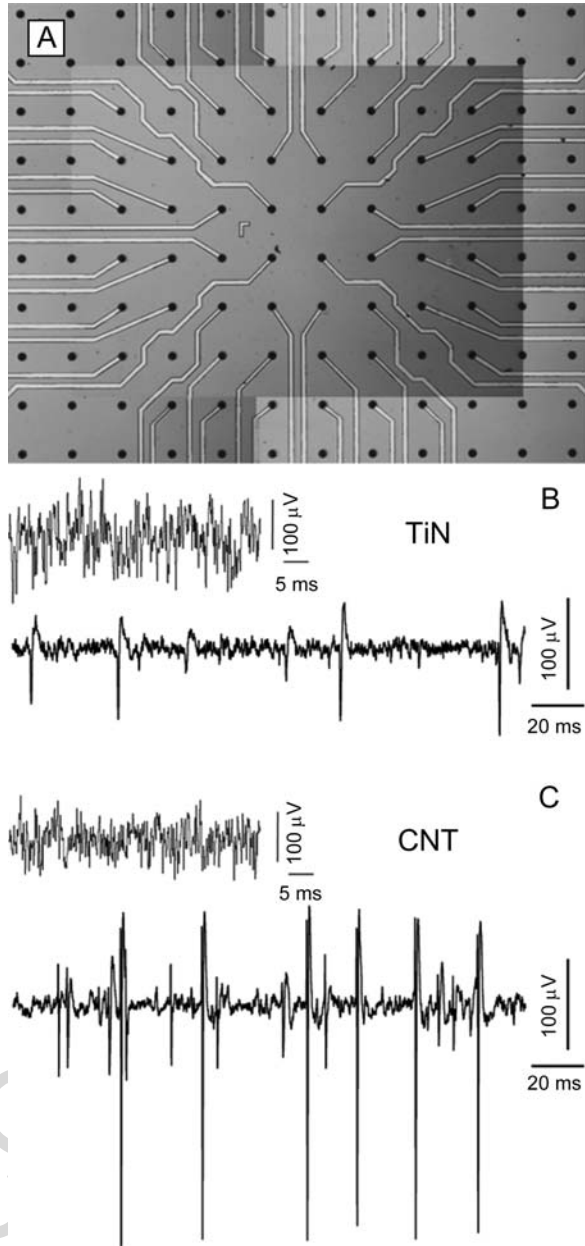


264 **Fig. 11.3** Vertically aligned carbon nanofibers (VACNFs) forming MEA record spontaneous electrical activity within the slice. (a) Individually addressable VACNF electrodes were arranged in a linear array (light micrograph). (b) An individual VACNF electrode assumes cone-like geometry (electron micrograph). (c) A hippocampal slice on a VACNF MEA (light micrograph). (d) Spontaneous action potential discharges/firing from a slice recorded by MEA is sensitive to tetrodotoxin (TTX; the time point of application indicated by the vertical dashed line), a blocker of voltage-gated Na^+ channels, confirming a neuronal source for spontaneous activity. Modified from [18], with permission
 265
 266
 267
 268
 269
 270

271 [see detailed comparison on p. 2190 of Ref. [18]]; the average noise level was
272 inversely proportional to the electrode dimensions. The recording noise level of
273 VACNF MEAs assessed in solution was favorable to enable extracellular record-
274 ings from cultured organotypic hippocampal slices. Prior to use of VACNF MEA
275 for recordings from slices, the chips were treated with a mixture of cell adhesion
276 permissive substrates poly-l-lysine and laminin to aide the adherence of slices to the
277 chip. Slices cultured separately were then applied onto chips (Fig. 11.3c) and were
278 held in place using a nylon mesh. Spontaneous electrical activity was simultane-
279 ously recorded in CA3 pyramidal and dentate gyrus granule cell layers; this activity
280 could be blocked by tetrodotoxin, a blocker of voltage-gated Na^+ channels underly-
281 ing action potentials producing spikes in the recordings (Fig. 11.3d). Conversely, the
282 removal of the inhibitory inputs by the addition of bicuculline, a blocker of gamma-
283 amino butyric acid receptors type A, resulted in epileptiform activity. In addition
284 to recording of spontaneous neuronal electrical activity, the application of stimuli
285 between two VACNF electrodes resulted in evoked field potentials. Taken together,
286 this study demonstrated that VACNF-based MEAs can deliver stimuli to the tis-
287 sue and record from it with improved spatial control compared to CNT films. The
288 three-dimensional (3D) cone-like protrusions offer recordings from single units with
289 amplitudes doubled from those seen in metal-based MEAs [19]. A lingering issue
290 with the use of VACNF-based MEA, shared with conventional metal-based elec-
291 trodes, is the rigidity of their surfaces. Namely, neural cells display sensitivity to the
292 mechanical stiffness of the scaffold [20, 21]. Consequently, to improve the use of
293 VACNF MEAs, Nguyen-Vu et al. [22] implemented VACNF brush-like electrodes
294 that have been additionally coated with the conductive polymer polypyrrole (PPy).
295 Such co-deposition approach found applications when using CNTs for recordings
296 of neuronal activity in vivo [see below Ref. [23]].

297 Shoval et al. [24] implemented the use of MWNT MEAs, which were produced
298 and packaged as previously reported [25], to record from whole-mount retinas.
299 Here, the deposition of CNTs onto titanium nitride (TiN) patterned substrate results
300 in highly conductive and porous/rough CNT islands/electrodes with low impedance
301 [25], which represent a good cell-adhesive surface as neurons entangle into a 3D
302 CNT matrix [26]. Bare TiN electrodes were designed to be porous achieving high
303 surface area and low impedance as well. Freshly isolated whole mount retinas were
304 placed onto MEAs with the retinal ganglion cells (RGCs) layer facing down. It
305 should be noted that RGCs represent the output cells from the retina encoding
306 the information transfer to the cortex by the frequency of their action potential
307 discharges. In many of the retinal dystrophies, these cells may remain intact to
308 transmit information, while photoreceptors degenerate. Consequently, there is an
309 urge to develop retinal implants that would by pass photoreceptors and directly
310 opto-electrically couple to RGC. Nonetheless, whole-mount retinas were restrained
311 onto chips using a polyester membrane filter. For comparison two chips were used:
312 bare TiN MEAs and MEAs containing additional coating with CNTs. In both cases,
313 some of the CNT or TiN islands on the chip were not electrically accessible, thus
314 do not represent any of the 60 active electrodes within the MEA (Fig. 11.4a).
315 These “spare” islands appear to assist in stabilizing the whole tissue. All islands

316 **Fig. 11.4** Electrical
 317 recordings of neural activity
 318 from the whole-mount retina
 319 using an MWNT MEA.
 320 (a) CNTs islands (*black dots*)
 321 deposited onto titanium
 322 nitride (TiN) patterned
 323 substrate. Note that not all
 324 CNT island are electrically
 325 active, since they are not
 326 connected to individual leads.
 327 (b–c) Recordings obtained
 328 from a whole-mount retina
 329 using a bare TiN and an
 330 MWNT-coated hybrid
 331 electrode, respectively. Top
 332 traces in b and c represent
 333 baseline noise level, while
 334 lower traces disclose
 335 spontaneous discharges of
 336 action potentials from retinal
 337 ganglion cells. Modified from
 338 [24], with permission



357 were 30 μm in diameter and spaced 200 μm apart; CNT islands had heights of
 358 several μm . Electrical recordings from retinas indicate that both types of electrodes
 359 can record spontaneous activity with RGCs discharging burst of action potentials (Fig. 11.4b and c). Individual electrodes of both types of MEAs appeared to
 360 record from at least two RGCs simultaneously as two sets of signal amplitudes

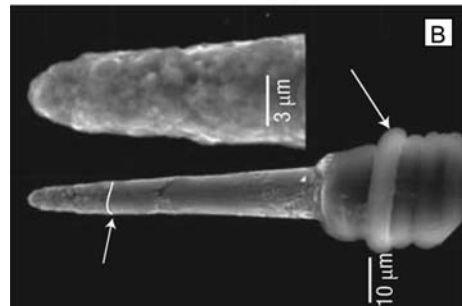
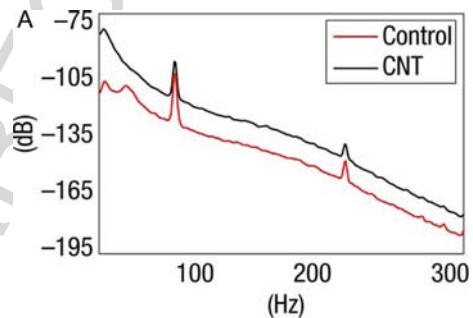
361 were clearly designated. The quality of recordings, however, were much better with
362 CNT-coated electrodes, as evidenced by decreased levels of baseline noise to half of
363 that seen in TiN electrodes and by more than doubled amplitudes of recorded action
364 potential amplitudes, resulting in a exceptionally high signal-to-noise ratio of the
365 CNT-coated electrode and clear single unit recordings (Fig. 11.4c, high amplitude
366 signals). Over time (minutes to hours) the number of electrodes that could record
367 RGCs activity increased on both type of chips. The amplitude of action potentials
368 recorded from TiN electrodes were stable, while recordings from CNT-coated
369 electrodes kept improving over time, showing enhanced amplitudes of recorded
370 action potentials with a 2% per minute increase; recordings lasted up to several
371 hours. This time-dependent improvement in recordings made by CNT-coated elec-
372 trodes could be attributed to improved coupling between electrodes and the tissue.
373 Moreover, the stimulation proof-of-concept experiments were executed. Stimulation
374 via an individual CNT-coated electrode (80 μm in diameter) can be used to record
375 evoked action potentials generally on a single neighboring electrode (200 μm spac-
376 ing). Taken together, the results of this study indicate that CNT-based MEAs have
377 promise for use in vivo.

378 Keefer et al. [23] established a procedure to coat planar and 3D electrodes with
379 MWNTs and compared their performances with the uncoated electrodes using cul-
380 tured neurons, the motor cortex of anaesthetized rats, and the V4 region of the visual
381 cortex of a conscious trained monkey. The initial experiments were done on plan-
382 ar MEAs in the absence of any brain cells. Deposition of CNTs on indium-tin
383 oxide based MEAs reduced the impedance of electrodes by ~ 20 fold and increased
384 the charge transfer by ~ 45 fold. Follow-up experiments used dissociated cultures
385 of frontal cortical neurons plated onto MEAs with bare gold surfaces or MEAs
386 containing an additional coating with CNTs. Both gold and CNT surfaces were
387 permissive substrates for neuronal growth. Spontaneous activity of the established
388 neuronal networks could be recorded for up to 3 months in culture with similar
389 success with either of MEA. However, the stimulation delivered via CNT-coated
390 MEAs was more effective than that of the bare gold-based MEAs, a finding consis-
391 tent with the CNTs' ability to lower impedance and increase charge transfer. One
392 consequence of such an effect by the CNTs was a decrease in noise levels by $\sim 65\%$,
393 which led to the increased sensitivity of CNT-coated MEAs, without a change in
394 their selectivity. These proof-of-principle experiments using planar MEAs were fol-
395 lowed by 3D electrodes and work in vivo. Commercially available 3D tungsten
396 and stainless steel sharp electrodes were over-coated with CNTs. Once again, when
397 tested in solution, these electrodes outperformed the bare metal electrodes by offer-
398 ing lower impedance and higher charge transfer. This performance could be further
399 enhanced if CNTs were co-deposited with conductive polymers such as PPy which
400 itself has been previously proven successful in experiments in vivo [27]. Two dif-
401 ferent animal models were used to test CNT-coated sharp electrodes: motor cortex
402 (controlling limb movement) of anesthetized rats and V4 cortex (involved in per-
403 ception of form-with-color) of an awake trained monkey. In experiments with rats,
404 two parallel electrodes, referred to as stereotrodes, one coated with CNTs and the
405 other bare tungsten, spaced apart by 125 μm , were used. For experiments with the
monkey cortex, the animal's task was to look at a flashing color square

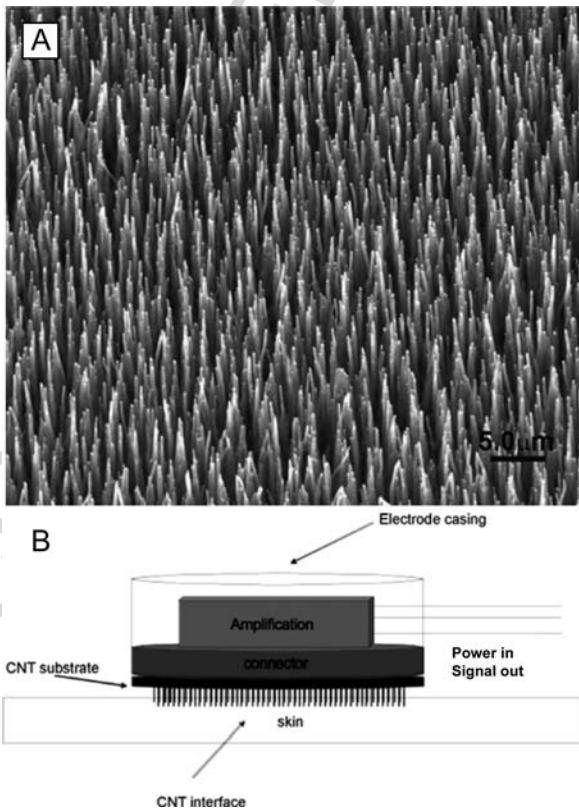
(form-with-color) on a screen, while recordings were performed using “stereotrodes” spaced 1 mm apart and containing one uncoated stainless steel (control) and another CNT-coated electrode (Fig. 11.4). In both in vivo experimental models, CNT-coated electrodes outperformed their paired control electrodes in terms of reduced noise (~17 dB) and increased sensitivity of detection (on average 7.4 dB more power) of spontaneous electrical neuronal activity throughout various ranges of acquisition frequencies (1–1000 Hz) relevant to brain (patho)physiology (Fig. 11.5a). As one would predict from their mechanical strength, CNTs endured the advancement of electrodes through the dura mater and remained intact even after recordings were completed, as assessed by electron microscopic investigation of the used electrodes (Fig. 11.5b). Taken together the coating of planar and 3D electrodes with CNTs allowed for their enhanced performance while recording neuronal electrical events in culture and in vivo. Thus, these hybrid electrodes could now be readily tested in exciting ongoing projects in the field of brain-machine interfaces, such as, the restoration of movement in tetraplegia [28]. Of course this should not occur with adequate testing for biosafety of CNT-based devices.

Thus far, we outlined the development of CNT-based electrodes used in direct contact with neural cells/brain tissue. However, it is commonly accepted that the safest way to record neural electrical activity is by using the EEG, since it is non-invasive procedure where electrodes are placed on a scalp. The location of such electrodes in humans is about 2–3 cm away from the surface of the cortex so that the electrical signal has low amplitude. Consequently, EEG recordings are generated by a rather large population of neural cells that are synchronously active. It

Fig. 11.5 CNT-coated electrodes record electrical activity in the primate visual cortex. (a) Power spectra obtained from CNT-coated and bare (control) metal electrodes indicate enhanced performance by CNT-coated electrodes. (b) CNT-coated electrode after recording from the monkey cortex. While insulating thin layer is peeled back (right arrow) from its original near the tip position (white line, left arrow) during penetration through the dura mater, the covalently attached CNTs at the electrode tip remain intact (inset). Modified from [23], with permission



451 should be noted that in addition to neuronal signals, the current flow created by
452 glial cells contributes to the EEG. For example, glial Müller cell potentials have
453 a time course similar to a component in the electroretinogram, referred to as the b
454 wave [29]. Additional consequence of low amplitude measurements presents itself
455 in the skin preparation for EEG recordings, which requires the use of electrolytic
456 gels and takes several minutes per electrode. Owing to the diffusion of such gels
457 into the skin, there is an additional requirement for stabilization of recordings. To
458 overcome some of these limitations, Ruffini et al. [30] developed a dry electrophysio-
459 logic sensor based on MWNTs to record the EEG from humans. Arrays of MWNTs
460 were grown on silicon disks to form brush like structures (Fig. 11.6a); individual
461 MWNTs were 50 nm in diameter and 10–15 μm length/height. Disks containing
462 an array of MWNTs were then diced into squares (1 × 1 cm) and mounted onto
463 commercial active electrodes with on-site amplification (Fig. 11.6b). As a standard
464 for comparison, conventional electrodes were used. Both types of electrodes were
465 connected to a commercial research electrophysiology recording system. Prior to the
466 use on human, a series of tests were run on a pig skin to record test signals applied
467 beneath the skin. Here, commercial electrodes were applied using an electrolytic
468 gel, while CNT-based electrodes were applied “dry” without skin preparation. The
469
470



483 **Fig. 11.6** MWNT-based
484 electrode for EEG. (a)
485 Scanning electron microscope
486 image of an array of MWNTs
487 grown on a silicon disk,
488 which can be mounted onto a
489 commercial active electrode
490 with on-site amplification (b).
491 (b) Schematics of CNT-based
492 EEG electrode. MWNT array
493 penetrates a superficial layer
494 of the skin owing to the
495 height/length of CNTs.
Modified from [30], with
permission

496 results showed similar performance of two types of electrodes. It should be noted,
497 however, that CNT-based electrodes only penetrated the superficial layer of skin
498 owing to the MWNT length/height. They caused neither pain nor any skin reaction
499 as reported by a human subject who was subjected to EEG recordings when dry
500 CNT and wet commercial electrodes were placed next to each other on the scalp for
501 comparison of their performances. The recordings were done simultaneous using
502 both types of electrodes using the protocol that encompassed spontaneous EEG and
503 event-related potentials (ERP). Spontaneous EEG consisted of two periods, one with
504 eyes open and the other with eyes shut, where the subject did not perform a task,
505 allowing recording of β and α waves, respectively. ERP were tested in response to
506 an auditory stimulus. In all conditions, dry CNT electrodes performed similarly to
507 the commercially available state of the art research-oriented wet electrodes.
508
509
510

511 **11.4 Biosafety of CNTs**

512
513 The promising and exciting possibilities for the use of CNTs in biomedical applica-
514 tions also raise concerns about their safety and exposure limits [reviewed in Refs.
515 [31, 32]]. Besides the above described use of CNTs in electrodes for neural inter-
516 faces, they are also emerging as a tool for targeted drug delivery [reviewed in Ref.
517 [33]] and, in this context, understanding of their biodistribution and biostability
518 is necessary. This knowledge could also be relevant to the applications of CNTs
519 in neural interfaces, since there is a possibility that CNTs could leach out from
520 electrodes and get distributed systemically if they can pass the blood-brain barrier
521 (BBB). Biodistribution of a variety of functionalized SWNTs indicate that, follow-
522 ing their delivery to the circulation, their blood retention can vary between 1 hour
523 and 1 day, depending on the animal model used and modifications of SWNTs; the
524 excretion/clearance of SWNTs via biliary and renal pathways is evident [34–37].
525 Interestingly, the biodistribution of CNTs in the brain 24 hours after their intra-
526 venous injection is much lower than that in the spleen and lungs, although these
527 organs are all highly vascularized, suggesting that the intact BBB can effectively
528 shield the entrance of CNTs into the brain [35]. Conversely, whether the BBB pre-
529 vents CNTs that leach out from implanted electrodes in the brain to exit into the
530 circulation has not yet been determined. However, even if this proves to be a clear-
531 ance pathway, CNTs available in the circulation would be at very low quantities, so
532 that such a scenario highly likely represents a trivial issue. Consequently, a pressing
533 concern presents itself in the possible direct effects that CNTs may have on neural
534 cells, which they contact as being an integral part of CNT-based electrodes.

535 The current literature on safety exposure limits and toxicity of CNTs on neural
536 cells is limited. Most of the CNT toxicity studies were done using non-neural cells
537 or cell-lines; these in vitro studies reported that the exposure to CNTs increased
538 oxidative stress and cell death in a dose-dependent manner [38–43]. However, some
539 of these studies were performed in such a manner that they do not directly address
540 the toxicity effect solely attributed to CNTs. For instance, the synthesis of CNTs

541 often involves the use of a metal catalyst, in which the residual content in CNTs
542 could be responsible for some of the observed toxic effects. Hence, non-purified
543 CNTs, containing higher content of a metal catalyst, have been shown to be more
544 potent in inducing oxidative stress in macrophages than the purified CNTs [44, 45].
545 Nonetheless, the length of CNTs can contribute to differential cellular response.
546 The degree of inflammatory response to subcutaneously applied CNTs *in vivo* was
547 greater for 825 nm in length CNTs than for shorter 220 nm in length CNTs [46].
548 It should be noted, however, that no severe inflammatory response, such as necro-
549 sis, was observed around both CNTs examined. Therefore, an evaluation of CNTs' *in vivo*
550 effect on cells/tissue must take into consideration the type of CNTs and the presence
551 of impurities.

552 The development of CNT-based materials for biomedical applications is still at
553 its infancy, and it is timely to investigate effects of CNTs on neural cells/tissue
554 before CNT-based devices become wide-spread in use. A recent *in vitro* study
555 showed that CNTs are biocompatible with neural cells [47]. However, a more sys-
556 tematic approach, using a variety of CNTs, is needed to address acute and long-term
557 effects that CNTs may have on the brain and the whole living organism in order to
558 establish safety guidance for the use of this promising nanomaterial in biomedical
559 applications in the near future.

560
561

562 11.5 Concluding Remarks and Future Directions

563

564
565 The intent of this chapter was to review the use of CNT-based neural interfaces for
566 stimulation and monitoring of neuronal activity. Owing to unique physical prop-
567 erties of this nanomaterial, CNT-based electrodes have potential to replace bare
568 metal electrodes for many of the medical applications, most notably brain-machine
569 interfaces. Further improvement in CNT-based electrodes may include their chem-
570 ical modifications, so they can detect various transmitters [discussed in Ref. [48]].
571 However, the use of CNT-based electrodes in human subjects must not occur without
572 adequate testing. It is encouraging that systemic administration of CNTs [36] indi-
573 cates that this form of carbon does not have any deleterious effect on mammalian
574 health. This pilot study could be used as a springboard to determine safe exposure
575 limits, both general and brain-specific, in humans. From the stance of implantation
576 in the brain, the chronic response of the tissue to the resident CNT-based electrodes
577 will have to be compared to the "classical" electrodes that have been in use for
578 decades [49]. Although the retention of CNTs on planar electrodes over the period
579 of ~3 months has been demonstrated [23], similar studies will need to be performed
580 with the CNT-coated 3D electrode arrays using even longer implantation times,
581 before we can make a full assessment of CNTs biocompatibility.

582

583 **Acknowledgements** We thank J. Robert Grammer for his comments on previous versions of this
584 manuscript. The authors' work is supported by a grant from the National Institute of Mental Health
585 (MH 069791) and National Science Foundation (CBET 0943343). We dedicate this chapter to the
late Glenn I. Hatton, whose work inspired new views of astrocyte-neuronal interactions.

References

1. Bekyarova E, Haddon RC, Parpura V. Biofunctionalization of Carbon Nanotubes, In: Kumar CSSR (ed) *Biofunctionalization of Nanomaterials (Nanotechnologies for the Life Sciences)*. Wiley-VCH, Weinheim-Berlin, Germany, 2005; pp. 41–71
2. Bekyarova E, Ni Y, Malarkey EB, et al. Applications of Carbon Nanotubes in Biotechnology and Biomedicine. *J Biomed Nanotechnol* 2005; 1:3–17
3. Qin L-C, Zhao X, Hirahara K, et al. The smallest carbon nanotube. *Nature* 2000; 408:50
4. Wang N, Tang ZK, Li GD, et al. Single-walled 4 A carbon nanotube arrays. *Nature* 2000; 408:50–51
5. Zheng LX, O’Connell MJ, Doorn SK, et al. Ultralong single-wall carbon nanotubes. *Nat Mater* 2004; 3(10):673–676
6. Cogan SR. Neural stimulation and recording electrodes. *Annu Rev Biomed Eng* 2008; 10:275–309
7. Krishnan A, Dujardin E, Ebbesen TW, et al. Young’s modulus of single-walled nanotubes. *Phys Rev B* 1998; 58(20):14013–14019
8. Schwartz AB, Cui XT, Weber DJ, et al. Brain-controlled interfaces: movement restoration with neural prosthetics. *Neuron* 2006; 52(1):205–220
9. Liopo AV, Stewart MP, Hudson J, et al. Biocompatibility of native and functionalized single-walled carbon nanotubes for neuronal interface. *J Nanosci Nanotechnol* 2006; 6(5): 1365–1374
10. Mazzatenta A, Giugliano M, Campidelli S, et al. Interfacing neurons with carbon nanotubes: electrical signal transfer and synaptic stimulation in cultured brain circuits. *J Neurosci* 2007; 27(26):6931–6936
11. Cellot G, Cilia E, Cipollone S, et al. Carbon nanotubes might improve neuronal performance by favouring electrical shortcuts. *Nat Nanotechnol* 2009; 4(2):126–133
12. Gheith MK, Pappas TC, Liopo AV, et al. Stimulation of neural cells by lateral layer-by-layer films of single-walled currents in conductive carbon nanotubes. *Adv Mater* 2006; 18(22):2975–2979
13. Kam NWS, Jan E, Kotov NA. Electrical stimulation of neural stem cells mediated by humanized carbon nanotube composite made with extracellular matrix protein. *Nano Lett* 2009; 9(1):273–278
14. Lovat V, Pantarotto D, Lagostena L, et al. Carbon nanotube substrates boost neuronal electrical signaling. *Nano Lett* 2005; 5(6):1107–1110
15. Wang K, Fishman HA, Dai HJ, et al. Neural stimulation with a carbon nanotube microelectrode array. *Nano Lett* 2006; 6(9):2043–2048
16. Mattson MP, Haddon RC, Rao AM. Molecular functionalization of carbon nanotubes and use as substrates for neuronal growth. *J Mol Neurosci* 2000; 14(3):175–182
17. Hu H, Ni YC, Montana V, et al. Chemically functionalized carbon nanotubes as substrates for neuronal growth. *Nano Lett* 2004; 4(3):507–511
18. Yu Z, McKnight TE, Ericson MN, et al. Vertically aligned carbon nanofiber arrays record electrophysiological signals from hippocampal slices. *Nano Lett* 2007; 7(8): 2188–2195
19. Heuschkel MO, Fejtl M, Raggenbass M, et al. A three-dimensional multi-electrode array for multi-site stimulation and recording in acute brain slices. *J Neurosci Meth* 2002; 114(2): 135–148
20. Balgude AP, Yu X, Szymanski A, et al. Agarose gel stiffness determines rate of DRG neurite extension in 3D cultures. *Biomaterials* 2001; 22(10):1077–1084
21. Discher DE, Janmey P, Wang YL. Tissue cells feel and respond to the stiffness of their substrate. *Science* 2005; 310(5751):1139–1143
22. Nguyen-Vu TD, Chen H, Cassell AM, et al. Vertically aligned carbon nanofiber architecture as a multifunctional 3-D neural electrical interface. *IEEE Trans Biomed Eng* 2007; 54(6 Pt 1): 1121–1128

- 631 23. Keefer EW, Botterman BR, Romero MI, et al. Carbon nanotube coating improves neuronal
632 recordings. *Nat Nanotechnol* 2008; 3(7):434–439
- 633 24. Shoval A, Adams C, David-Pur M, et al. Carbon nanotube electrodes for effective interfacing
634 with retinal tissue. *Front Neuroengineering* 2009; 2(4):8
- 635 25. Gabay T, Ben-David M, Kalifa I, et al. Electro-chemical and biological properties of carbon
636 nanotube based multi-electrode arrays. *Nanotechnology* 2007; 18(3):035201 (6pp)
- 637 26. Sorkin R, Gabay T, Blinder P, et al. Compact self-wiring in cultured neural networks. *J Neural*
638 *Eng* 2006; 3(2):95–101
- 639 27. Cui X, Wiler J, Dzaman M, et al. In vivo studies of polypyrrole/peptide coated neural probes.
640 *Biomaterials* 2003; 24(5):777–787
- 641 28. Hochberg LR, Serruya MD, Friehs GM, et al. Neuronal ensemble control of prosthetic devices
642 by a human with tetraplegia. *Nature* 2006; 442(7099):164–171
- 643 29. Miller RF, Dowling JE. Intracellular responses of the Muller (glial) cells of mudpuppy retina:
644 their relation to b-wave of the electroretinogram. *J Neurophysiol* 1970; 33(3):323–341
- 645 30. Ruffini G, Dunne S, Fuentemilla L, et al. First human trials of a dry electrophysiology sensor
646 using a carbon nanotube array interface. *Sensors and Actuators a-Physical* 2008; 144(2):
647 275–279
- 648 31. Helland A, Wick P, Koehler A, et al. Reviewing the environmental and human health
649 knowledge base of carbon nanotubes. *Environ Health Perspect* 2007; 115(8):1125–1131
- 650 32. Stern ST, McNeil SE. Nanotechnology safety concerns revisited. *Toxicol Sci* 2008; 101(1):
651 4–21
- 652 33. Klumpp C, Kostarelos K, Prato M, et al. Functionalized carbon nanotubes as emerging
653 nanovectors for the delivery of therapeutics. *Biochim Biophys Acta* 2006; 1758(3):404–412
- 654 34. Cherukuri P, Gannon CJ, Leeuw TK, et al. Mammalian pharmacokinetics of carbon nanotubes
655 using intrinsic near-infrared fluorescence. *Proc Natl Acad Sci USA* 2006; 103(50):
656 18882–18886
- 657 35. Liu Z, Cai W, He L, et al. In vivo biodistribution and highly efficient tumour targeting of
658 carbon nanotubes in mice. *Nat Nanotechnol* 2007; 2(1):47–52
- 659 36. Liu Z, Davis C, Cai W, et al. Circulation and long-term fate of functionalized, biocompatible
660 single-walled carbon nanotubes in mice probed by Raman spectroscopy. *Proc Natl Acad Sci*
661 *USA* 2008; 105(5):1410–1415
- 662 37. Singh R, Pantarotto D, Lacerda L, et al. Tissue biodistribution and blood clearance rates of
663 intravenously administered carbon nanotube radiotracers. *Proc Natl Acad Sci USA* 2006;
664 103(9):3357–3362
- 665 38. Cui D, Tian F, Ozkan CS, et al. Effect of single wall carbon nanotubes on human HEK293
666 cells. *Toxicol Lett* 2005; 155(1):73–85
- 667 39. Manna SK, Sarkar S, Barr J, et al. Single-walled carbon nanotube induces oxidative stress
668 and activates nuclear transcription factor-kappaB in human keratinocytes. *Nano Lett* 2005;
669 5(9):1676–1684
- 670 40. Monteiro-Riviere NA, Nemanich RJ, Inman AO, et al. Multi-walled carbon nanotube
671 interactions with human epidermal keratinocytes. *Toxicol Lett* 2005; 155(3):377–384
- 672 41. Jia G, Wang H, Yan L, et al. Cytotoxicity of carbon nanomaterials: single-wall nanotube,
673 multi-wall nanotube, and fullerene. *Environ Sci Technol* 2005; 39(5):1378–1383
- 674 42. Bottini M, Bruckner S, Nika K, et al. Multi-walled carbon nanotubes induce T lymphocyte
675 apoptosis. *Toxicol Lett* 2006; 160(2):121–126
43. Magrez A, Kasas S, Salicio V, et al. Cellular toxicity of carbon-based nanomaterials. *Nano Lett* 2006; 6(6):1121–1125
44. Kagan VE, Tyurina YY, Tyurin VA, et al. Direct and indirect effects of single walled carbon nanotubes on RAW 264.7 macrophages: role of iron. *Toxicol Lett* 2006; 165(1):88–100
45. Pulskamp K, Diabate S, Krug HF. Carbon nanotubes show no sign of acute toxicity but induce intracellular reactive oxygen species in dependence on contaminants. *Toxicol Lett* 2007; 168(1):58–74

- 676 46. Sato Y, Yokoyama A, Shibata K, et al. Influence of length on cytotoxicity of multi-walled
677 carbon nanotubes against human acute monocytic leukemia cell line THP-1 in vitro and
678 subcutaneous tissue of rats in vivo. *Mol Biosyst* 2005; 1(2):176–182
- 679 47. Dubin RA, Callegari GC, Kohn J, et al. Carbon nanotube fibers are compatible with
680 mammalian cells and neurons. *IEEE Trans Nanobiosci* 2008; 7(1):11–14
- 681 48. Parpura V. Instrumentation: carbon nanotubes on the brain. *Nat Nanotechnol* 2008; 3(7):
682 384–385
- 683 49. Hubel DH. Tungsten microelectrode for recording from single units. *Science* 1957;
684 125(3247):549–550
- 685
- 686
- 687
- 688
- 689
- 690
- 691
- 692
- 693
- 694
- 695
- 696
- 697
- 698
- 699
- 700
- 701
- 702
- 703
- 704
- 705
- 706
- 707
- 708
- 709
- 710
- 711
- 712
- 713
- 714
- 715
- 716
- 717
- 718
- 719
- 720